Prediction of attachment line transition for a high-lift wing based on two-dimensional flow calculations with RANS-solver

Jochen Wild[1] and Oliver T. Schmidt[2]

[1] DLR Braunschweig, Institute of Aerodynamics and Flow Technology, Lilienthalplatz 7, D-38108 Braunschweig, Germany, jochen.wild@dlr.de
[2] TU Berlin, ILR, Marchstraße 12-14, D-10587 Berlin, Germany, Oliver.T.Schmidt@TU-Berlin.de

Summary

This investigation shows that the properties of the two-dimensional flow around a high-lift multi-element airfoil obtained by solving the Reynolds-averaged Navier-Stokes equations can be used for the prediction of attachment-line transition (ALT) by the criterion of Pfenninger. Flow calculations are performed for three spanwise sections of a three-dimensional swept and tapered high-lift wing for which the occurrence of ALT is assumed at higher Reynolds numbers. It is shown that the onset of ALT is predicted reliably for changes of the angle of attack. The method is also applicable to indicate the spanwise location where ALT occurs first.

1 Introduction

The aerodynamic performance of a high-lift wing in terms of lift coefficient is coupled to the development of the boundary layer on the slat as it influences the effective curvature through viscous displacement. Hereby the occurrence of ALT on the slat of a high-lift wing can be responsible for a limit of the aerodynamic performance with increasing Reynolds number.

Without ALT the boundary layer starting from the attachment line downstream to the suction peak is laminar due to the acceleration of the flow and transition occurs slightly behind the suction peak at the earliest. In this case, with increasing Reynolds number, the boundary layer thickness decreases resulting in a higher effective curvature and therefore more suction and an increasing lift coefficient. In contrast the occurrence of ALT results in an overall turbulent boundary layer with increased thickness and therefore reduced effective curvature. This leads to reduced suction at the leading edge of the slat and a reduced high-lift performance in terms of lift coefficient is observed.

The existence of the phenomenon of ALT was first discovered by Gray [5]. Pfenninger conducted further investigations with the emphasis on avoiding ALT [9, 10, 11].These experiments led to a criterion, described below, that was assumed to characterize the occurrence of ALT. Experimental investigations by Poll [12, 13]

and Arnal and Juillen [1, 2] validated this criterion for the assumption of infinite swept wings. Newer experiments of Seraudie et. al. [14] also verified the criterion for swept finite high-lift wings at high angles of attack. In addition to the wind tunnel experiments mentioned above flight tests also show the relevance of the criterion [9, 4].

Starting point of this investigation are measurements of the ProHMS high-lift wing-body half-model of a transport aircraft in the cryogenic wind tunnel Cologne DNW-KKK for a Reynolds number range of $Re_\infty = 1.4 \times 10^6 \ldots 6.2 \times 10^6$ [15]. With increasing Reynolds number the maximum lift coefficient of the high-lift configuration decreased after having reached a maximum at a medium Reynolds number of $Re_\infty = 3.0 \times 10^6$. This led to the assumption that ALT occurs above $Re_\infty = 3.0 \times 10^6$. Since transition measurements were not performed, the attempt is made to predict the occurrence of ALT by numerical methods.

Instead of computing the whole three dimensional flow field, here the attempt is made to use only two-dimensional flow calculations of selected wing sections. There are at least two reasons for this approach: a) the two-dimensional flow calculations are cheaper in terms of computational resources and easier to set up; b) due to the fact that high-lift design is still mainly performed based on two-dimensional computations a validated prediction method based on this data can be easily implemented into the design process, giving hints to avoid ALT.

2 Attachment-Line Transition Prediction

The prediction criterion for the onset of ALT of Pfenninger [9] used within this work distinguishes between the flow normal to the leading edge and the crossflow. It correlates the crossflow velocity outside the boundary layer w with the acceleration of the flow out of the stagnation line $\frac{\partial u_e}{\partial s}$. Pfenninger formulates an attachment line boundary layer Reynolds number

$$Re_{\theta_{a.l.}} = 0.405 \frac{w}{\sqrt{\nu \frac{\partial u_e}{\partial s}}} \tag{1}$$

with the kinematic viscosity ν, the local arc length s in the coordinate system normal to the leading edge and the velocity component at the edge of the boundary layer normal to the leading edge u_e.

A number of experiments on swept wings and cylinders (e.g. of Pfenninger [11] and Poll [13]) verified a lower limit of $Re_{\theta_{a.l._{krit.}}} = 100$ below which no ALT occurs. Experiments of Arnal [1] with a swept wing at incidence showed, that due to the limited extent of the wing an upper critical value of $Re_{\theta_{a.l._{krit.}}} = 133$ exists. Between both values existing turbulence is only propagated, above the value of Arnal the turbulence is amplified. All investigations showed that the main mechanism for ALT in real applications is the propagation of turbulence from upstream along the attachment line, the so called bypass transition or leading edge contamination. Transition due to instabilities, which may occur at higher values of $Re_{\theta_{a.l.}}$ as has

been shown experimentally by Poll [13] and has also been computed by Joslin [6, 7] using direct numerical simulation, has never been observed for real aircraft.

As can be seen from (1) the only term that takes into account three-dimensional flow is the crossflow velocity w outside the viscous flow, which for an infinite swept and untapered wing is constant

$$w = U_\infty sin\phi \tag{2}$$

with the onflow velocity U_∞ and the sweep angle ϕ. All other terms of eq. 1 correspond to the flow components normal to the leading edge. By assuming that the effects of tapering and the limited span of the wing only play a minor role for the most part of a high aspect ratio wing, this criterion for ALT can be based on the evaluation of calculations of the flow normal to the leading edge.

3 Flow Calculation

For the calculation of the flow the structured DLR RANS-solver FLOWer [8] is used. It solves the unsteady compressible Reynolds-averaged Navier-Stokes equations in applying an explicit 5-stage Runge-Kutta time-stepping method. Turbulence modeling is done using the Spalart-Allmaras model with Edwards-modification. The turbulence equations are solved using a fully implicit scheme that allows for high CFL numbers.

In order to minimize grid dependencies of the flow solution, separate grids are generated using the DLR grid generator MegaCads [3] for each wing section at each Reynolds number. In particular the boundary layer resolution is adjusted in order to have approximately the same resolution in terms of the number of cells in the boundary layer and to obtain a value of the dimensionless wall distance y^+ on the order of 1.

For this investigation three spanwise sections of the wing of the ProHMS high-lift model are used, denoted inboard, midboard and outboard, corresponding to the pressure tab rows of the model. They are each located in the middle of the slat elements, far enough from any model tracks, so that 2D flow assumptions are most likely to apply.

In order to perform 2D calculations comparable with the 3D flow the assumption of an infinite swept wing is used. This leads to a scaling of the wing section into a coordinate system normal to the leading edge

$$y_{2D} = z_{3D}/cos\phi\,.^1 \tag{3}$$

Now only the onflow components normal to the leading edge are of interest

$$\begin{gathered} Ma_{\infty_{2D}} = Ma_{\infty_{3D}} cos\phi,\ Re_{\infty_{2D}} = Re_{\infty_{3D}} cos^2\phi, \\ \alpha_{2D} = atan\left(\frac{tan\alpha_{3D}}{cos\phi}\right). \end{gathered} \tag{4}$$

[1] in 3D usually the z-coordinate points in the vertical direction while in 2D the y-coordinate is used and $z_{2D} = 0$.

To compare coefficients of 2D calculation and 3D experiment an additional scaling applies due to the scaled onflow

$$c_{p_{3D}} = c_{p_{2D}} cos^2\phi, C_{L_{3D}} = C_{L_{2D}} cos^2\phi. \quad (5)$$

It is a priori unknown if the flow around the slat leading edge is turbulent or laminar. Only for conditions where ALT has already occured at a lower Reynolds number fully turbulent flow can be assumed. For all other conditions two calculations are performed, the first fully turbulent, the second with a prescribed laminar region on the slat lower side fixing transition at the slat leading edge. All other wing elements are calculated fully turbulent in all cases.

4 Correlation method

The main issue when comparing two-dimensional data of a wing section with data from the three-dimensional wing is that a priori the local angle of attack for the wing section is unknown as long as no spanwise lift distributions are available. To be able to compare the data it is necessary to find the right 2D data for the corresponding 3D data. Throughout this work a comparison is done based on the measured and computed pressure distributions. Calculations are performed for distinct angles of attacks, and afterwards the experimental data is screened to find a corresponding angle of attack of the 3D high-lift wing where the pressure distributions match. Since this is not exact for the whole wing, primarily the pressure distributions on the slat are considered for comparison.

Fig. 1 shows such a correlation for each of the three sections, where the calculated 2D pressure distribution is plotted against the pressure distribution of the 3D experiment for $Re_{\infty_{3D}} = 6.0 \times 10^6$. It can be seen that the pressure distributions match the experiment especially on the slat. The biggest deviations can be seen for the midboard section for the rear part of the main element and the flap. The pressure distributions of the experiment indicate attached flap flow, while the flap flow is separated in the calculations. This might be a result of the fully turbulent calculation of the main element and the flap, since the transition locations are not known and the effort of transition prediction is not undertaken. The increased boundary layer thickness around the flap tends to slightly close the effective gap, which leads together with the increased friction losses to a separation of the flap. Another reason for the differences may be that the local sweep angle in the rear part of the high-lift wing is different from the angle assumed for the normalization due to the taper of the wing. This is observed especially on the flap in the different levels of stagnation pressures. Nevertheless the slat pressure distribution is matched very well, and since the slat flow is the primary interest in this investigation, all cases in the following are treated using the described method.

5 Results

A first point of interest is if the predicted occurrence of ALT correlates with the dependency of the lift coefficient on the onflow Reynolds number. Since it is in all

likelihood the occurrence of ALT on the slat influencing the lift coefficient behavior, in the following only the slat is regarded. Fig. 2 shows the lift coefficient of the 3D measurements over the Reynolds number for a fixed angle of attack of $\alpha_{3D} = 15°$ together with the corresponding calculated values of $R_{\theta_{a.l.}}$ for the three sections. It is observed that with increasing Reynolds number the lift coefficient decreases. There are two major changes in the slope of $C_{L_{3D}}$ vs. $Re_{\infty_{3D}}$ that correspond to $Re_{\theta_{a.l.}}$ to the first and last wing section exceeding the upper limit of $Re_{\theta_{a.l.krit.}} = 133$. Thus it can be seen that the predicted occurrence of ALT is in accordance with the measured effect on the lift coefficient. Summarizing it is proposed that the prediction of ALT by using 2D calculations can be applied.

The ALT criterion for the slat is expected to be highly sensitive to the angle of attack due to the variation of the attachment line position. For low incidences the attachment line is known to be at the leading edge while at high angles of attack the attachment line moves upstream towards the lower trailing edge of the slat. On the other hand the region of maximum suction is located at the leading edge where the curvature of the slat is the highest. So the distance between attachment line and suction peak varies as does the suction itself. The development of $Re_{\theta_{a.l.}}$ with respect to the local 2D angle of attack is shown for the inboard section in fig. 3, for the midboard section in fig. 4 and for the outboard section in fig. 5. The general trend is an increasing value of $Re_{\theta_{a.l.}}$ with increasing angle of attack. The only case where $Re_{\theta_{a.l.}}$ is decreasing is for high α_{2D} for the inboard and midboard section, where the flow indicates being beyond $C_{L_{max}}$.

For the evaluation of ALT occurrence it is worthwhile to investigate at which spanwise section ALT begins. Fig. 6 shows the values of $Re_{\theta_{a.l.}}$ over the relative wing span $\eta = y/b$ for a specific angle of attack $\alpha_{3D} = 15°$ at different onflow Reynolds numbers. Fig. 7 shows the same for a specific Reynolds number $Re_{\infty_{3D}} = 3 \times 10^6$ at different angles of attack. It is observed that ALT starts at the outboard section propagating towards the inboard region with increasing Reynolds number and angle of attack.

6 Conclusion

The present investigation is an attempt to predict the 3D flow phenomenon of attachment line transition on the slat of a transport aircraft in high-lift configuration through two-dimensional flow calculations of distinct wing sections. This was expected to be possible as the unknown values of the used ALT criterion of Pfenninger correspond to the flow normal to the leading edge. It has been shown that the predicted occurrence of ALT correlates to the measured behavior of the lift coefficient for the ProHMS 3D half model. The method reliably predicts the onset of ALT when changing the angle of attack and gives an indication of the spanwise section at which ALT occurs first.

Acknowledgments

The authors would like to thank Airbus Germany GmbH for the supply oft he 3D high-lift model and data. embedded in the joint projects ProHMS and ProHMS+. They would also like to thank H. W. Stock for sharing his experience in transition prediction.

References

[1] Arnal., D., Juillen, J.: Leading-edge contamination and relaminarization on a swept wing at incidence. In Cebeci, T., ed.: Numerical and Physical Aspects of Aerodynamic Flows. Springer-Verlag Berlin Heidelberg (1990) 391–402

[2] Arnal, D., Juillen, J., Reneaux, J., Gasparian, G.: Effect of wall scution on leading edge contamination. Aerospace Science and Technology **1** (1997) 505–517

[3] Brodersen, O., Hepperle, M., Ronzheimer, A., Rossow, C.C., Schöning, B.: The parametric grid generation system megacads. In Soni, B., Thompson, J., Häuser, J., Eiseman. P., eds.: 5th International Conference on Numerical Grid Generation in Computational Field Simulation, National Science Foundation (NSF) (1996) 353–362

[4] van Dam, C., Los, S., Miley, S., Rooock, V., Yip, L., Bertelrud, A., Vijgen, P.: In-fligh boundary-layer state measurements on a high-lift system: Slat. Journal of Aircraft **34**, (1997) 748–756

[5] Gray, W.: The effect of wing sweep on laminar flow, TM 255, RAE(1953)

[6] Joslin, R.: Simulation of three-dimensional symmetric and asymmetric instabilities in attachment-line boundary layers. AIAA Journal **34** (1996) 2432–2434

[7] Joslin, R.: Simulation of nonlinear inb1abilities in an attachment-line boundary layer. Fluid Dynamics Research **18** (1996) 81–97

[8] Kroll, N., Rossow, C.C., Becker, K., Thiele, F.: Megaflow – a numerical flow simulation system. Proceedings 1998-2.7.4, ICAS(1998)

[9] Pfenninger, W.: Flow phenomena at the leading edge of swept wings. AGARDograph 97, AGARD (1965) Part IV.

[10] Pfenninger, W., Bacon jr., J.W.: Amplified laminar boundary layer oscillations and transition at the front attachment line of a 45° swept flat-nosed wing with and without boundary layer suction. In Wells, C., 00.: Viscous Drag Reduction, Plenum Press New York (1969)

[11] Pfenninger, W.: Laminar flow control – laminarization. Report AGARD-R-654, AGARD (1977)

[12] Poll, D.: Three-dimensional boundary layer transition via the mechanism of "attachment line contamination" and "cross flow instability". In Eppler, R., Fasel, H., eds.: Laminar-Turbulent Transition. Springer-Verlag Berlin Heidelberg New York (1979) 253–262

[13] Poll, D.: Some observations of the transition process on the windward face of a long yawed cylinder. Journal of Fluid Mechanics **150** (1985) 329–356

[14] Séraudie, A., Perraud, J., Moens, F.: Transition measurement and analysis on a swept wing in high lift configuration. Aerospace Science and Technology **7** (2003) 569–576

[15] Wild, J., Puffert-Meissner, W., Sitzmann, M., Lekemark, L.: Messung des FNG Hochauftriebs-Modells bei hohen Reynoldszahlen im Kryogenischen Windkanal Köln. DLR-IB 124-2003/37, DLR (2003)

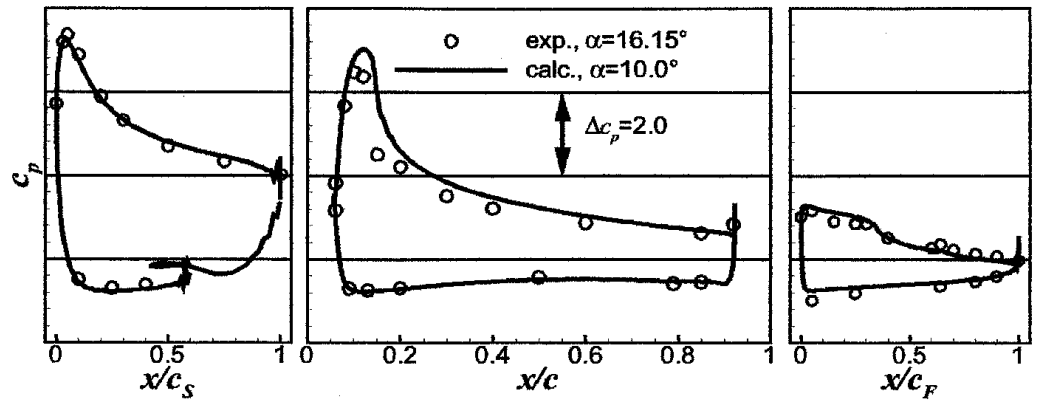

(a) inboard section

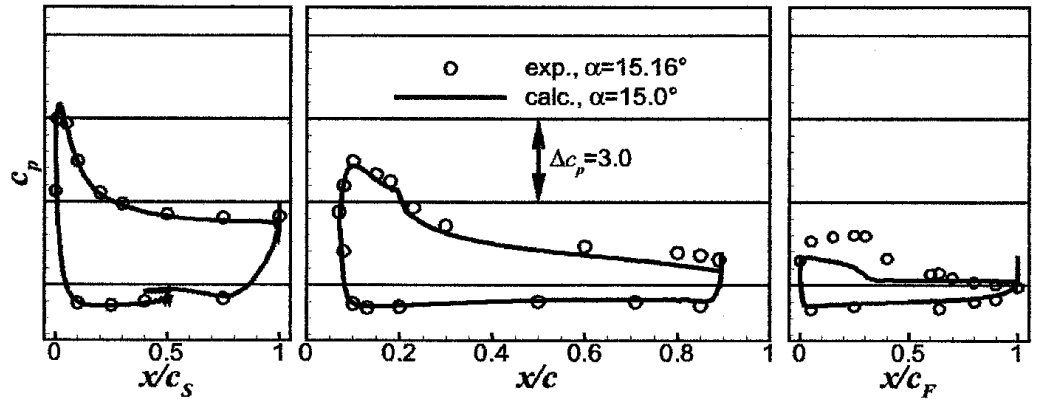

(b) midboard section

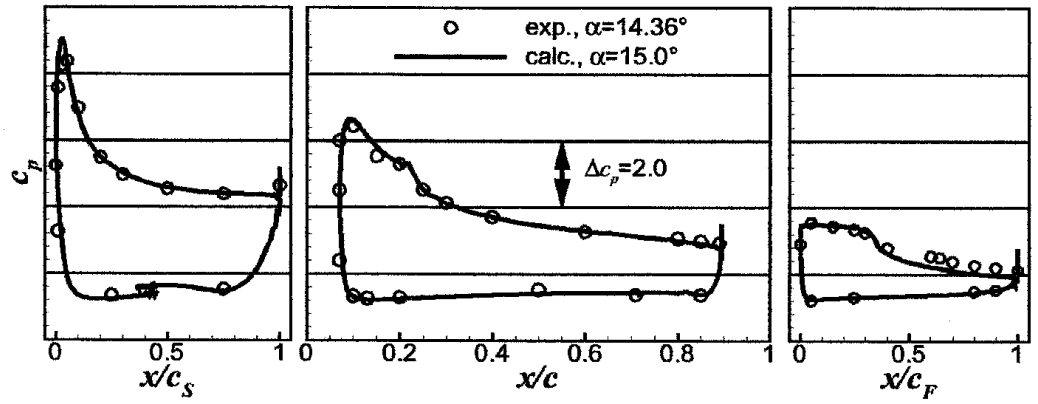

(c) outboard section

Figure 1 Correlation of calculated 2D pressure distributions with experimental data for $Re_{\infty_{3D}} = 6.0 \times 10^6$

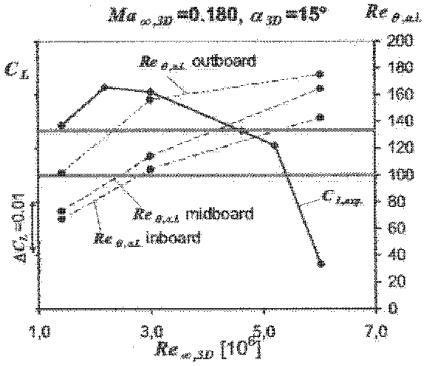

Figure 2 Variation of the lift coefficient and the attachment line Reynolds number with the onflow Reynolds number for $\alpha_{3D} = 15°$

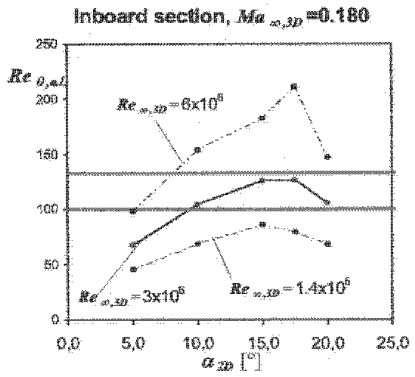

Figure 3 Variation of the attachment line Reynolds number with the local angle of attack for the inboard section

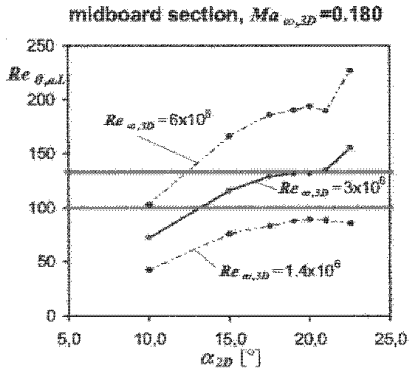

Figure 4 Variation of the attachment line Reynolds number with the local angle of attack for the midboard section

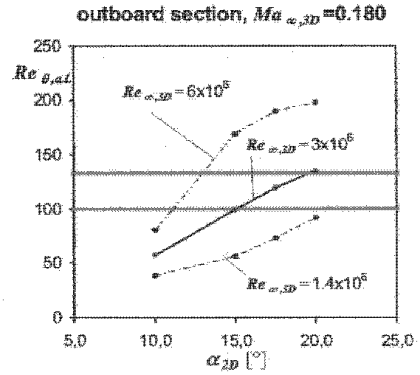

Figure 5 Variation of the attachment line Reynolds number with the local angle of attack for the outboard section

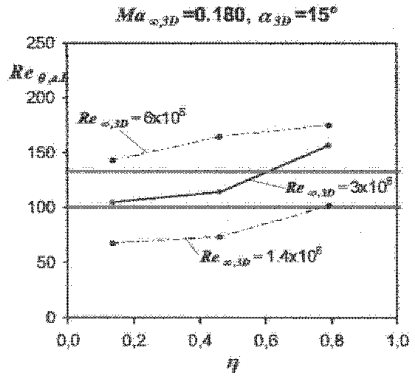

Figure 6 Spanwise variation of $Re_{\theta_{a.l.}}$ with the onflow Reynolds number for $\alpha_{3D} = 15°$

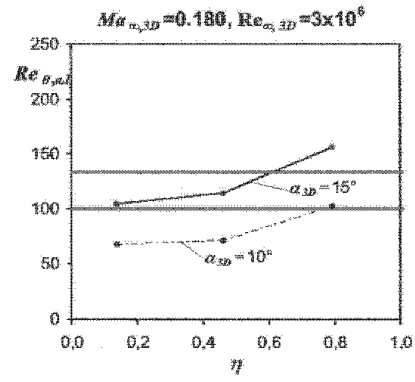

Figure 7 Spanwise variation of $Re_{\theta_{a.l.}}$ with the angle of attack for $Re_{\infty_{3D}} = 3 \times 10^6$